https://doi.org/10.5194/amt-2022-333
Preprint. Discussion started: 31 January 2023


Atmospheric Measurement Techniques Discussions

# A compact formulation for the retrieval of the overlap function in an elastic/Raman aerosol lidar

Adolfo Comerón[1], Constantino Muñoz-Porcar[1], Alejandro Rodríguez-Gómez[1], Michaël Sicard[1,2], Federico Dios[1], Cristina Gil-Díaz[1], Daniel Camilo Fortunato dos Santos Oliveira[1], Francesc Rocadenbosch[1,2]

[1]CommSensLab-UPC, Universitat Politècnica de Catalunya, 08034 Barcelona, Spain.

[2]Ciències i Tecnologies de l'Espai-Centre de Recerca de l'Aeronàutica i de l'Espai/Institut d'Estudis Espacials de Catalunya (CTE-CRAE/IEEC), Universitat Politècnica de Catalunya, 08034 Barcelona, Spain.

*Correspondence to*: Alejandro Rodríguez-Gómez (alejandro.rodriguez.gomez@upc.edu)

**Abstract.** We derive an explicit (i.e. non-iterative) formula for the retrieval of the overlap function in an aerosol lidar with both elastic and Raman $N_2$ or/and $O_2$ channels used for independent measurements of aerosol backscatter and extinction coefficients. The formula requires only the measured, range-corrected, elastic and the corresponding Raman signals, plus an assumed lidar ratio. We assess the influence of the lidar ratio error in the overlap function retrieval and present retrieval examples.

## 1. Introduction

At near ranges, lidar signals suffer from the uncomplete overlap between the emitted laser beam and the field of view of the receiving optical assembly. This occurs because a part of the rays that arrive at the telescope aperture from short- range illuminated volumes do not pass the receiver field stop and do not reach the detector. The overlap function of a lidar system can be defined as the range-resolved ratio of the number of photons reaching a channel detector to the total number of photons arriving at the telescope aperture (Comeron et al., 2011). This ratio is a function of distance and depends on the optical and geometrical arrangement of the transmitting and receiving optics of the instrument. The key parameters determining the overlap function are those related to the laser beam features (diameter, shape and divergence), to the receiver optical properties (telescope diameter, focal length and field stop diameter) and to the relative location and alignment between transmitter and receiver optical axes (Halldórsson and Langerholc, 1978), (Lefrère, 1982). The overlap function is usually zero at the telescope aperture level and progressively grows up to one at the so-called full-overlap range, where all the incident backscattered radiation, or at least a constant proportion of it, is collected by the receiving optics and reaches the photodetector.

The existence of an uncomplete overlap prevents the system to provide trustfully lidar signals for ranges below the full-overlap altitude, thus limiting the minimum operational range of the lidar instrument. To overcome these overlap issues, some systems duplicate their receivers, enabling both far- and near-range telescopes and detectors and combining their respective signals for reconstructing a lidar signal with an extended (towards the lower end) full overlap range. For example, Polly$^{XT}$ systems (Engelmann et al., 2016) use this type of solution and their full overlap altitude is reduced down to ~100 m. Alternatives when such a hardware-based extension of the operational range is not possible rely on the calculation or estimation of the overlap function and on the correction of the detected signals from the effect of the incomplete overlap. Several works have developed theoretical calculations of the overlap function using the transmitter and the receiver optical parameters, both on analytical basis (e.g. (Comeron et al., 2011)) and relying on ray tracing procedures (e.g. (Kumar and Rocadenbosch, 2013)). However, such theoretical approaches are in many cases not practical because most of the system parameters in which they are based are not easily measurable ~~or estimated~~ (Kokkalis, 2017) and they change, sometimes unpredictably and unnoticeably, with time. Alternatives to theoretical calculations are based on experimental estimations relying on practical field lidar measurements and inversions. A first proposal, presented by Sasano et al in 1978 (Sasano et al., 1979), is based on the assumption of homogeneous atmosphere up to distances above the full overlap altitude. In many cases, this method is not practical, first, because its applicability depends on the state of the atmosphere and second, because in order to assure the required atmospheric homogeneity, it demands for a horizontal alignment of the lidar line-of-sight that is not always possible. Up to date, the best-established and most widely accepted method was presented by Wandinger and Ansmann (Wandinger and Ansmann, 2002). This approach assumes that the lidar system has a Raman channel to independently retrieve the aerosol extinction and relies on the fact that, under the reasonable

https://doi.org/10.5194/amt-2022-333
Preprint. Discussion started: 31 January 2023


Atmospheric Measurement Techniques Discussions

assumption of the same overlap function for the elastic and the Raman channels, the Raman inversion of the backscatter coefficient is not affected by the uncomplete overlap.

In this paper, we present an alternative formulation for the retrieval of the overlap function based on the same principles as the one discussed in (Wandinger and Ansmann, 2002), i.e. the fact that the backscatter coefficient retrieved by the Raman method is not affected by the uncomplete overlap. However, unlike in the Wandinger and Ansmann method, our formulation results in an explicit formula that does not require repeated inversions of the backscatter coefficient by both the Raman (Ansmann et al., 1992) and Klett (Klett, 1985), (Sasano et al., 1985) methods ~~in an iterative way~~. Section 2 develops the proposed formulation. In section 3 we assess the effect of an erroneous lidar ratio on the retrieved overlap function. Examples based on real measurements are presented in section 4. Conclusions and outlook are summed up in section 5.

## 2. Overlap retrieval

The proposed method uses, like ref. (Wandinger and Ansmann, 2002), the elastic and the Raman signals corresponding to one of the emitted wavelengths of an aerosol lidar measurement. First, let's consider the expression of the range-corrected elastic lidar signal, $X(R)$, affected by a partial overlap function, $O(R)$, where the aerosol and molecular components of the extinction coefficient is written using the corresponding lidar ratios, $S_{a0}(R)$ and $S_m = 8\pi/3$ sr respectively:

$$X(R) = A\,O(R)\left[\beta_{a0}(R)+\beta_{m0}(R)\right]\exp\left\{-2\int_0^R\left[S_{a0}(x)\beta_{a0}(x)+S_m\beta_{m0}(x)\right]dx\right\}, \quad (1)$$

where $A$ is an instrument constant, and $\beta_{a0}(R)$ and $\beta_{m0}(R)$ are respectively the aerosol and molecular components of the backscatter coefficient at the emitted wavelength $\lambda_0$. To avoid using the instrument constant, we look for an aerosol-free range, $R_m$, at which the aerosol backscatter coefficient can be assumed to be zero and where $\beta_{m0}(R_m)$ can be estimated from the pressure and the temperature provided by a radiosonde or by using a standard model of the atmosphere. Assuming as well that $O(R_m)=1$, we have at that range

$$X(R_m) = AO(R)\beta_{m0}(R_m)\exp\left\{-2\int_0^{R_m}\left[S_{a0}(x)\beta_{a0}(x)+S_m\beta_{mo}(x)\right]dx\right\}. \quad (2)$$

Dividing Eq. (1) by Eq. (2) and re-ordering terms, we obtain:

$$O(R)\left[\beta_{a0}(R)+\beta_{m0}(R)\right]\exp\left[-2\int_{R_m}^R S_{a0}(x)\beta_{a0}(x)dx\right] = \beta_{m0}(R_m)\frac{X(R)}{X(R_m)}\exp\left[2S_m\int_{R_m}^R\beta_{m0}(x)dx\right]. \quad (3)$$

Now we follow steps similar to those leading to the well-known Klett's formula (Klett, 1985), (Gimmestad and Roberts, 2010), but keeping explicitly the overlap function in the equations. Multiplying both members of Eq. (3) by $S_{a0}(R)\exp\left[-2\int_{R_m}^R S_{a0}(x)\beta_{m0}(x)dx\right]$, we obtain

$$O(R)S_{a0}(R)\left[\beta_{m0}(R)+\beta_{a0}(R)\right]\exp\left\{-2\int_{R_m}^R S_{a0}(x)\left[\beta_{a0}(x)+\beta_{m0}(x)\right]dx\right\} =$$

$$= \beta_{m0}(R_m)\frac{X(R)S_{a0}(R)}{X(R_m)}\exp\left\{2\int_{R_m}^R\left[S_m - S_{a0}(x)\right]\beta_{m0}(x)dx\right\}. \quad (4)$$

In the left-hand member of Eq. (4) we recognize that

$$S_{a0}(R)\left[\beta_{m0}(R)+\beta_{a0}(R)\right]\exp\left\{-2\int_{R_m}^R S_{a0}(x)\left[\beta_{a0}(x)+\beta_{m0}(x)\right]dx\right\} =$$

$$-\frac{1}{2}\frac{d}{dR}\exp\left\{-2\int_{R_m}^R S_{a0}(x)\left[\beta_{a0}(x)+\beta_{m0}(x)\right]dx\right\}, \quad (5)$$

https://doi.org/10.5194/amt-2022-333
Preprint. Discussion started: 31 January 2023


Atmospheric Measurement Techniques Discussions

with which Eq. (4) can be rewritten as

$$\frac{d}{dR}\exp\left\{-2\int_{R_m}^{R} S_{a0}(x)\left[\beta_{a0}(x)+\beta_{m0}(x)\right]dx\right\}=$$

$$-2\beta_{m0}(R_m)\frac{X(R)}{X(R_m)O(R)}S_{a0}(R)\exp\left\{2\int_{R_m}^{R}\left[S_m-S_{a0}(x)\right]\beta_{m0}(x)\,dx\right\} \tag{6}$$

Integrating both members of Eq. (6) between $R_m$ and $R$ and rearranging terms one obtains

$$\exp\left\{-2\int_{R_m}^{R} S_{a0}(x)\left[\beta_{a0}(x)+\beta_{m0}(x)\right]dx\right\}=$$

$$1-2\frac{\beta_{m0}(R_m)}{X(R_m)}\int_{R_m}^{R}\frac{X(x)}{O(x)}S_{a0}(x)\exp\left\{2\int_{R_m}^{x}\left[S_m-S_{a0}(x')\right]\beta_{m0}(x')\,dx'\right\}dx\,. \tag{7}$$

Substituting the right member of Eq. (7) for $\exp\left\{-2\int_{R_m}^{R} S_{a0}(x)\left[\beta_{a0}(x)+\beta_{m0}(x)\right]dx\right\}$ in the left-hand member of Eq. (4) and rearranging we arrive at

$$O(R)\left[\beta_{m0}(R)+\beta_{a0}(R)\right]=$$

$$\frac{\beta_{m0}(R_m)X(R)\exp\left\{2\int_{R_m}^{R}\left[S_m-S_{a0}(x)\right]\beta_{m0}(x)\,dx\right\}}{X(R_m)-2\beta_{m0}(R_m)\int_{R_m}^{R}\frac{X(x)}{O(x)}S_{a0}(x)\exp\left\{2\int_{R_m}^{x}\left[S_m-S_{a0}(x')\right]\beta_{m0}(x')\,dx'\right\}dx}\,. \tag{8}$$

Note that Eq. (8) is the Klett's solution of the lidar equation (Klett, 1985), (Sasano et al., 1985), except for the overlap function appearing in its left-hand member and in the integral in the denominator in its right-hand member.

Now, from the Raman inversion method we obtain, assuming that the overlap functions of both the elastic and the Raman channels are the same, a backscatter coefficient not affected by the incomplete overlap (Ansmann et al., 1992):

$$\beta_{a0}(R)+\beta_{m0}(R)=\frac{X(R)X_R(R_m)\beta_{m0}(R)}{X(R_m)X_R(R)}\frac{\exp\left\{-\int_{R}^{R_m}\left[\alpha_{a0}(x)+S_m\beta_{m0}(x)\right]dx\right\}}{\exp\left\{-\int_{R}^{R_m}\left[\alpha_{aR}(x)+S_m\beta_{mR}(x)\right]dx\right\}}\,, \tag{9}$$

with $X_R(R)$ the range-corrected Raman signal, and $\alpha_{aR}(R)$ and $\beta_{mR}(R)$ the aerosol-extinction and the molecular-backscatter coefficients respectively, both at the Raman-shifted wavelength $\lambda_R$. If we neglect the difference between the aerosol extinction coefficients at $\lambda_0$ *and* $\lambda_R$ and we divide Eq. (8) by Eq. (9) we arrive finally at the formula:

$$O(R)=\frac{\beta_{m0}(R_m)X(R_m)X_R(R)}{X_R(R_m)\beta_{m0}(R)}\cdot\frac{\exp\left\{2\int_{R_m}^{R}\left[S_{a0}(x)-S_m\right]\beta_{m0}(x)\,dx\right\}\exp\left\{\int_{R}^{R_m}S_m\left[\beta_{m0}(x)-\beta_{mR}(x)\right]dx\right\}}{X(R_m)-2\beta_{m0}(R_m)\int_{R_m}^{R}\frac{X(x)}{O(x)}S_{a0}(x)\exp\left\{2\int_{R_m}^{x}\left[S_{a0}(x')-S_m\right]\beta_{m0}(x')\,dx'\right\}dx}\,. \tag{10}$$

Eq. (10) could be solved iteratively for $O(R)$ by assuming an initial $O(R)$ in the right-hand member of Eq. (10) (e.g. $O(R)=1$, or the immediately previous overlap function assumed as valid for the system). This will give a new $O(R)$ estimate that would be substituted again in the right hand of Eq. (10), and the procedure will continue until $O(R)$ converges.

https://doi.org/10.5194/amt-2022-333
Preprint. Discussion started: 31 January 2023


Atmospheric Measurement Techniques Discussions

However, it is also possible to obtain an explicit expression for $O(R)$ by casting Eq. (10) into the form of a Volterra integral equation ((Mathews and Walker, 1970), section 11-5), which, in turn, can be converted into a first degree differential equation that can be integrated using standard techniques ((Mathews and Walker, 1970), section 1-1, see appendix for details). To do that, we call

$$f(R) = \frac{1}{O(R)} \tag{11}$$

and define the function $g(R)$, $\phi(R)$ and $\psi(R)$ as

$$g(R) = \frac{X_R(R_m)\beta_{m0}(R)}{\beta_{m0}(R_m)X_R(R)} \cdot \frac{1}{\exp\left\{2\int_R^{R_m}[S_{a0}(x)-S_m(x)]\beta_{m0}(x)dx\right\}\exp\left\{S_m\int_R^{R_m}[\beta_{m0}(x)-\beta_{mR}(x)]dx\right\}}, \tag{12}$$

$$\phi(R) = \frac{2X_R(R_m)\beta_{m0}(R)}{X(R_m)X_R(R)} \cdot \frac{1}{\exp\left\{2\int_R^{R_m}[S_{a0}(x)-S_m(x)]\beta_{m0}(x)dx\right\}\exp\left\{S_m\int_R^{R_m}[\beta_{m0}(x)-\beta_{mR}(x)]dx\right\}}, \tag{13}$$

and

$$\psi(R) = X(R)S_{a0}(R)\exp\left\{2\int_R^{R_m}[S_{a0}(x)-S_m]\beta_{m0}(x)dx\right\}. \tag{14}$$

Then, following the steps detailed in the appendix, one arrives at the explicit form of the overlap function

$$O(R) = \frac{\beta_{m0}(R_m)X_R(R)}{\beta_m(R)X_R(R_m)} \times \frac{\exp\left\{2\int_R^{R_m}[S_{a0}(x)-S_m]\beta_{m0}(x)dx\right\}\exp\left\{S_m\int_R^{R_m}[\beta_{m0}(x)-\beta_{mR}(x)]dx\right\}}{\exp\left\{2\frac{X_R(R_m)}{X_m}\int_R^{R_m}\frac{S_{a0}(x)\beta_{m0}(x)X(x)}{X_R(x)}\exp\left(-S_m\int_x^{R_m}[\beta_{m0}(x')-\beta_{mR}(x')]dx'\right)dx\right\}}. \tag{15}$$

Note that every term in Eqs. (10) and (15), except the aerosol lidar ratio profile $S_{a0}(R)$, can be obtained either directly from the elastic and Raman lidar signals ($X(R)$ and $X_R(R)$), or calculated from the pressure and temperature provided by a radiosonde or by using a standard model of the atmosphere ($\beta_{m0}(R)$ and $\beta_{mR}(R)$).

## 3. Influence of the lidar ratio

To assess the influence of the assumed lidar ratio on the overlap function retrieval we substitute in Eq. (10) the expressions of $X(R)$ and $X_R(R)$ that would correspond to a given aerosol distribution,

$$X(R) = AO(R)[\beta_{m0}(R)+\beta_{a0}(R)]\exp\left\{-2\int_0^R[\alpha_{a0}(x)+S_m\beta_{m0}(x)]dx\right\}, \tag{16a}$$

$$X_R(R) = BO(R)\beta_{mR}(R)\exp\left\{-\int_0^R[\alpha_{a0}(x)+\alpha_{aR}(x)]+S_m[\beta_{m0}(x)+\beta_{mR}(x)]\right\}dx, \tag{16a)b}$$

where $A$ and $B$ are instrument constants. We also assume that we may use an "erroneous" lidar ratio

$$S'_{a0}(R) = S_{a0}(R) + \Delta S_{a0}(R), \tag{17}$$

https://doi.org/10.5194/amt-2022-333
Preprint. Discussion started: 31 January 2023


Atmospheric Measurement Techniques Discussions

where $S_{a0}(R)$ is the "true" lidar ratio and $\Delta S_{a0}(R)$ the deviation from it. Using $S'_{a0}(R)$ in Eq. (15), replacing in it the expressions of $X(R)$ and $X_R(R)$ given by Eqs. (16a) and (16b) and assuming, as it was already done to obtain Eq. (10), that the aerosol extinctions at the excitation and Raman wavelengths are the same, i.e. $\alpha_{aR}(R) = \alpha_{a0}(R) = S_{a0}(R)\beta_{a0}(R)$, we find, after some boring and cumbersome, but otherwise straightforward, algebraic developments, the surprisingly simple result

$$O'(R) = O(R)\exp\left[-2\int_R^{R_m} \Delta S_{ao}(x)\beta_{ao}(x)dx\right] \quad (18)$$

where $O'(R)$ is the overlap function found, different from the true one, $O(R)$, because of the error $\Delta S_{a0}$ in the lidar ratio.

One reaches the following conclusions from Eq. (18):

a) If the atmosphere measured to retrieve the overlap function were aerosol-free, i.e. $\beta_{a0}(R) = 0$ for all ranges, the assumed lidar ratio (hence $\Delta S_{a0}$) would be irrelevant, since Eq. (18) would lead to $O'(R) = O(R)$.

b) Likewise, if there is no aerosol for a range $R_l < R < R_m$, in that range $O'(R) = O(R)$ regardless of the assumed lidar ratio.

c) If $\Delta S_{a0}(x) > 0$, then $O'(R) < O(R)$ in the range with aerosol.

d) If $\Delta S_{a0}(x) < 0$, then $O'(R) > O(R)$ in the range with aerosol.

Note that, because $\beta_{a0}$ tends to be larger at shorter wavelengths, the sensitivity of the retrieved overlap function to an error in the assumed lidar ratio is expected to be larger at shorter wavelengths.

## 4. Results

We have used Eq. (15) to obtain estimates of the overlap function at 355 nm and 532 nm of the Raman lidar of the Universitat Politècnica de Catalunya (UPC), an eight-channel multispectral Raman lidar that is fully described in (Kumar et al., 2011), with the modification in the UV branch of the wavelength separation unit described in ref. (Zenteno-Hernández et al., 2021) to implement a $N_2/O_2$ purely rotational Raman channel at 354 nm. This instrument belongs to the EARLINET European aerosol lidar network, currently integrated into the Aerosol, Clouds and Trace Gases Research Infrastructure (ACTRIS). To retrieve the overlap function at 355 nm, we have used the purely rotational Raman channel, which provides a higher signal-to-noise ratio than the vibro-rotational one (Zenteno-Hernández et al., 2021). For the overlap function at 532 nm we used the elastic signal return and the signal of the $N_2$ vibro-rotational Raman channel at 607 nm.

We have applied our method using two nighttime measurements (60-minute measurement on 11 November 2021 starting at 20:41 UTC and 60-minute measurement 1 December 2021 at 1:44). Fig. 1 presents the backscatter coefficients obtained with the Raman method (Eq. (9), no smoothing applied to the signals) at 355 nm and 532 nm neglecting the difference between the aerosol extinction coefficients. Note that this approximation is very well justified when the Raman channel is a purely rotational one, as in the case of the backscatter coefficient at 355 nm, since the two signals employed are at almost the same wavelength. Fig. 1 shows that the aerosol backscatter coefficient at both wavelengths was much lower for the 1st of December measurement than for the 11th of November one. It also shows that the backscatter coefficient for the same day is higher at the shorter wavelength. Fig. 1 warns also on a possible breakdown of the equal overlap function hypothesis for the elastic and Raman channels, more clearly seen examining the profiles of 1st of December: while the 532-nm aerosol backscatter coefficient shows a reasonable behavior until very low altitudes, the 355-nm one has a sudden fall below approximately 400 m. For this reason, in this particular case of optical alignment we should distrust the overlap function retrieval below that height.

https://doi.org/10.5194/amt-2022-333
Preprint. Discussion started: 31 January 2023


Atmospheric Measurement Techniques Discussions

Fig. 2 shows the results of the overlap function retrieval with our method for three "reasonable" lidar ratios (25 sr, 50 sr and 75 sr) from the 11th of November 2021 measurement. The reference height is taken at 5.5 km, where the Rayleigh fit of the signals indicate absence of aerosol (in agreement with the profiles of fig. 1). The detected lidar signal sequences are noisy, especially the Raman ones, whereas the overlap function cannot have steep or sudden variations at far ranges; therefore, a smoothing procedure, coupled with a Monte Carlo routine to assess the residual error bars, has been employed. An overlap profile retrieved with the original noisy sequences (only for 50 sr lidar ratio) is plotted as well.

The raw elastic and Raman signal sequences detected by our lidar were fitted to a Rayleigh reference profile obtained from a nearby radio-sound. The sequences were corrected in range as well, being all these processes common in lidar inversion techniques. The result of this process leads to $X(n)$ and $X_R(n)$, standing for elastic and Raman signal sequences. Previous ("noisy") estimates of the overlap profiles were calculated with these sequences.

These sequences were then smoothed to reduce the remaining noise, especially in the segments corresponding to high altitudes. This smoothing uses an adaptive sliding average approach. Each sample of the smoothed sequence was calculated as

$$X_{X\_sm}(n) = \frac{1}{L+1} \sum_{i=n-L/2}^{n+L/2} X_X(i), \tag{19}$$

where the sub-index $X$ stands for either elastic or Raman. The averaging window length $L$ varies from 1 to 150 (3.75 m to 562.5 m taking into account the raw range resolution of our lidar) as $n$ grows. For low altitudes (low $n$) the noise is not significant and the expected lidar signals show relevant variations, so $L$ must be short, while it can be made longer for sequence segments corresponding to farther ranges, especially in the molecular zone.

The noise of these signals is estimated by comparing the non-smoothed sequences with the smoothed one. The estimation of this noise is necessary to create the different realizations in a Monte Carlo strategy to compute the error bars of the overlap estimation. Considering that the sequences have been smoothed by performing a $(L+1)$-long average, the standard deviation of the n-th sample is estimated as (Papoulis and Pillai, 2002):

$$\Delta X_X(n) = \frac{1}{\sqrt{L+1}} \cdot \sqrt{\frac{1}{2L+1} \cdot \sum_{i=n-L}^{n+L} \left[ X_X(i) - X_{X\_sm}(i) \right]^2}. \tag{20}$$

The uncertainty of the calculated overlap profiles is estimated by using a common Monte Carlo approach. With the statistics obtained with equations (19) and (20), $N_{MC}$ (usually $N_{MC} \approx 100$) pairs of elastic and Raman signal statistically independent sequences are synthesized. Each of these synthesized sequences are generated as

$$X_{X\_k}(n) = X_{X\_sm}(n) + e_{X\_k}(n), \tag{21}$$

where each $e_{X\_k}(n)$ is a realization of a Gaussian random variable with zero average and standard deviation $\Delta X_X(n)$.

With these $N_{MC}$ sequence pairs, $N_{MC}$ overlap profiles $Ov_k(n)$ are calculated. The average overlap profiles $Ov(n)$ and error bars $\Delta Ov(n)$ presented in the next figures have been calculated as (Papoulis and Pillai, 2002):

$$Ov(n) = \frac{1}{N_{MC}} \sum_{k=1}^{100} Ov_k(n) \tag{22}$$

$$\Delta Ov(n) = \sqrt{\frac{\sum_{k=1}^{N_{MC}} \left[ Ov_k(n) - Ov(n) \right]^2}{(N_{MC} - 1)}} \tag{23}$$

https://doi.org/10.5194/amt-2022-333
Preprint. Discussion started: 31 January 2023


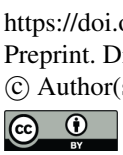

Atmospheric Measurement Techniques Discussions

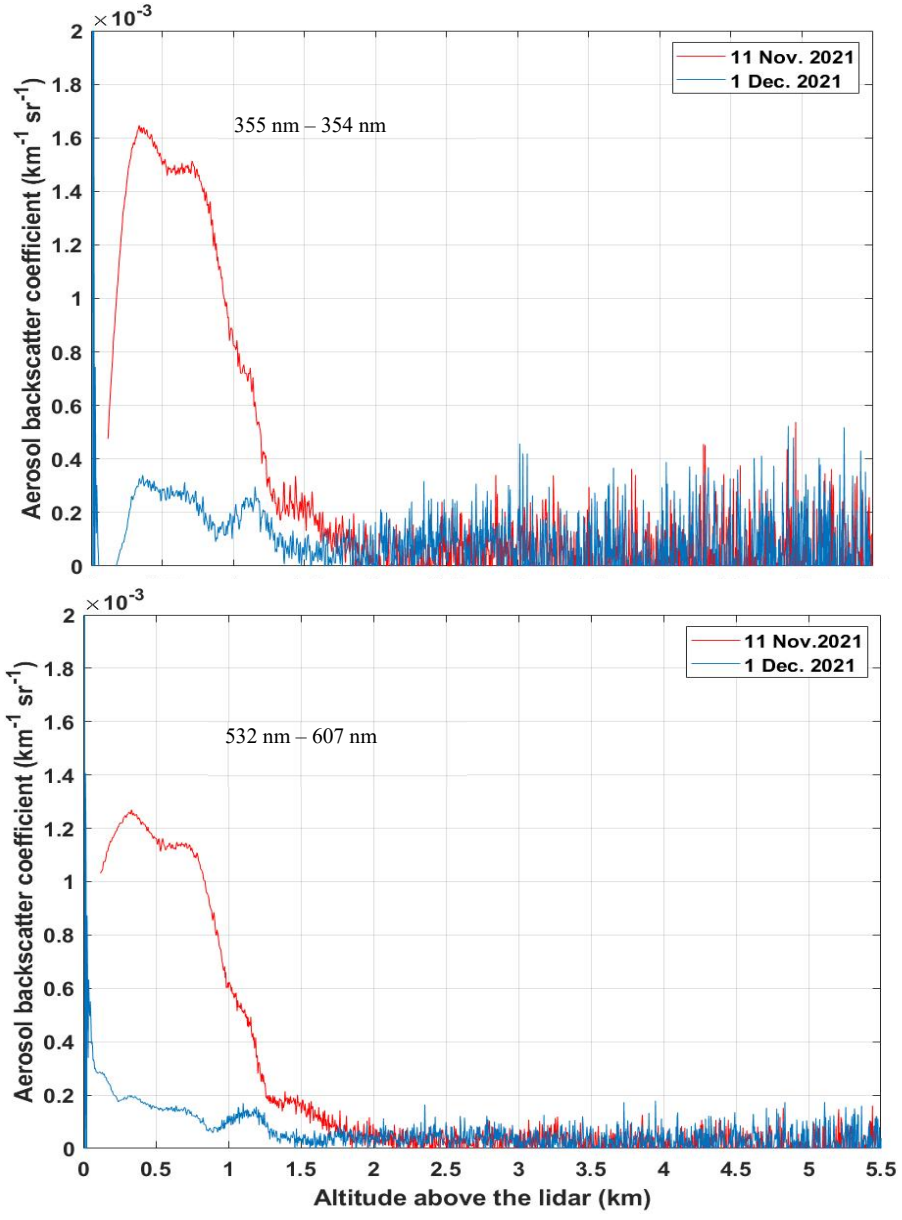


**Fig. 1. Aerosol backscatter coefficient using the Raman method formula. Upper graph: nominally at 355 nm using the 355 nm elastic channel and the 354 purely rotational channel. Lower graph: nominally at 532 nm using the 532 nm elastic channel and the 607 nm vibro-rotational Raman channel.**

https://doi.org/10.5194/amt-2022-333
Preprint. Discussion started: 31 January 2023


Atmospheric Measurement Techniques Discussions

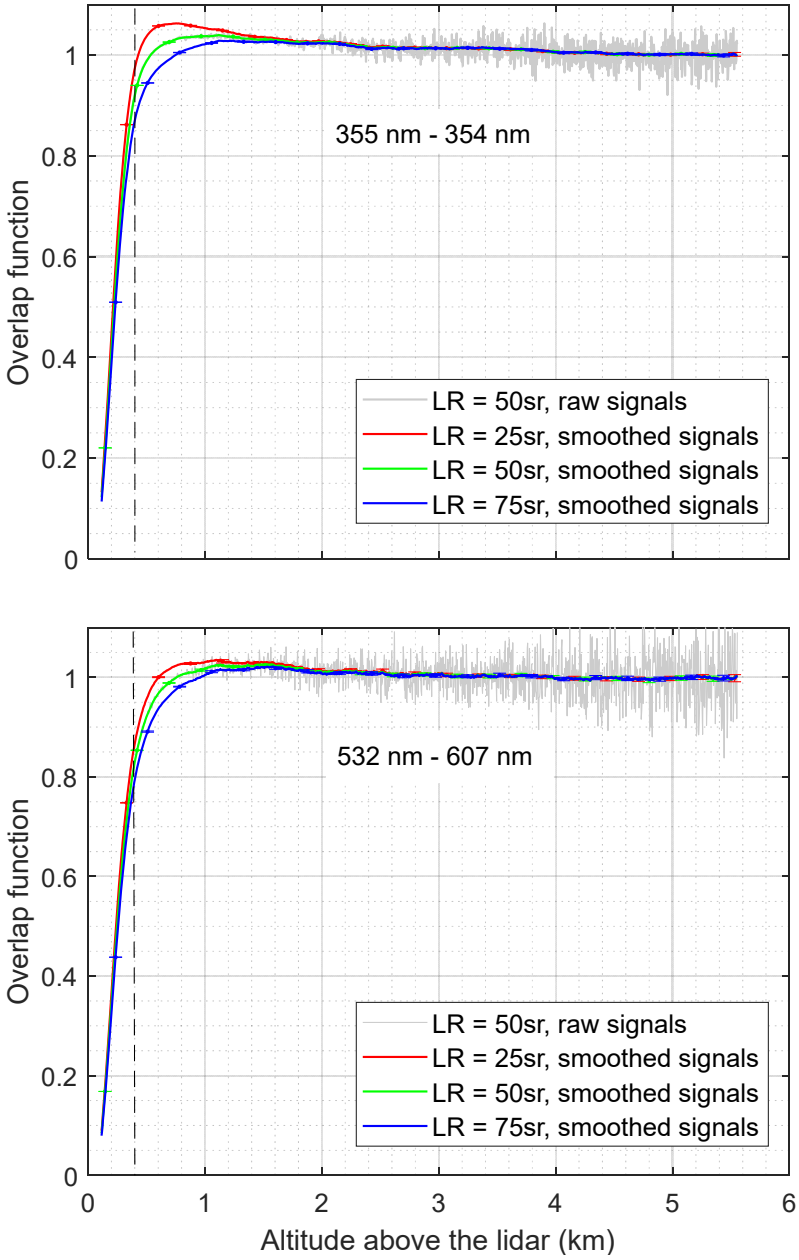


**Fig. 2. Overlap functions retrieved assuming different lidar ratios (LR) at 355 nm (upper panel) and 532 nm (lower panel) from measurements carried out on 11th of November 2021. A smoothing procedure described in the text has been applied and error bars are shown. As a reminder of the applied smoothing a raw result for a 50-sr lidar ratio is shown in grey. The vertical discontinuous line marks the 400-m height below which the correction is to be mistrusted.**

https://doi.org/10.5194/amt-2022-333
Preprint. Discussion started: 31 January 2023


Atmospheric Measurement Techniques Discussions

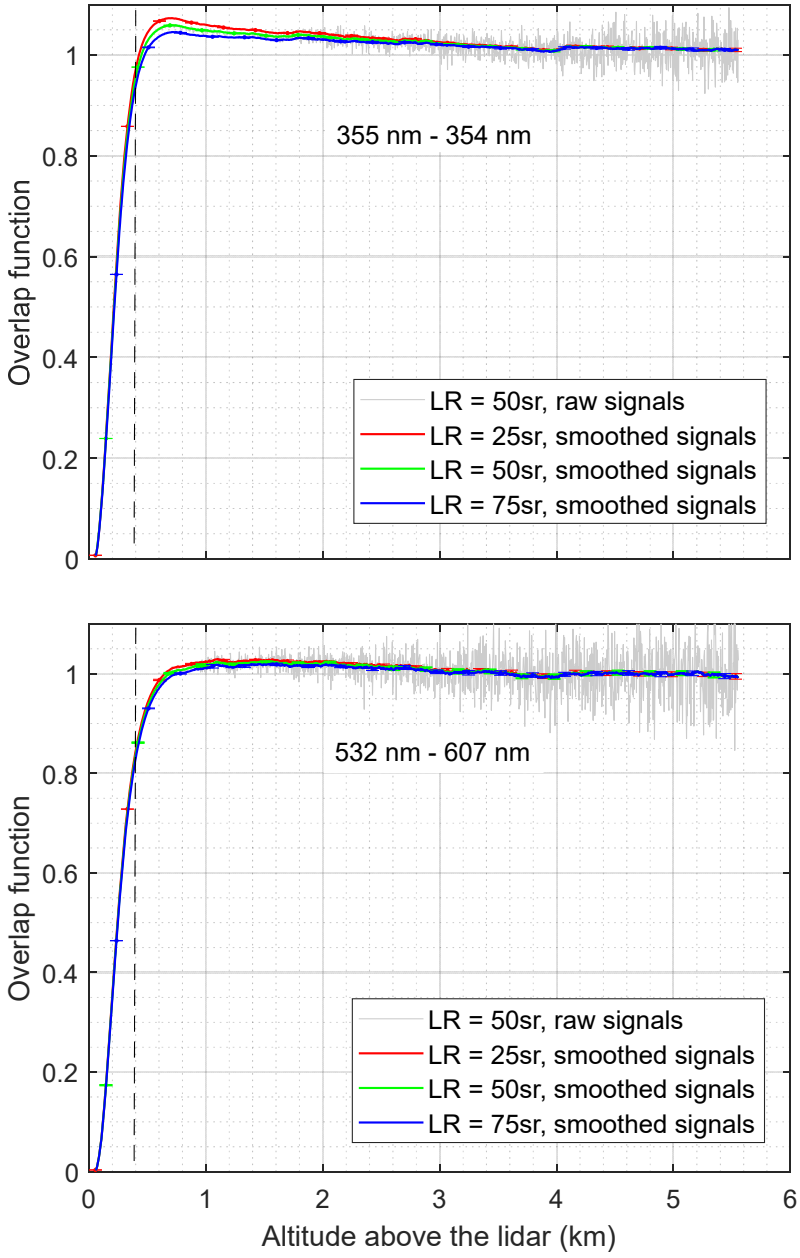


**Fig. 3. Overlap functions retrieved assuming different lidar ratios (LR) at 355 nm (upper panel) and 532 nm (lower panel) from measurements carried out on 1st of December 2021. The same smoothing procedure and method to obtain error bars as in fig. 2 have been employed. As in fig. 2, the vertical dashed line marks the range below which the retrieval is subject to caution. As a reminder of the applied smoothing a raw result for a 50-sr lidar ratio is shown in grey.**

https://doi.org/10.5194/amt-2022-333
Preprint. Discussion started: 31 January 2023


Atmospheric Measurement Techniques Discussions

In fig. 3 the retrieved overlap functions from data of the 1st of December 2021 are represented for the same assumed lidar ratios as in figure 2. As expected (section 3), being the aerosol backscatter coefficients at both wavelengths lower in this measurement, the difference between the overlaps obtained with different lidar ratios is lower than for the 11th of November. Also, because the backscatter coefficient at 532 nm is lower than at 355 nm, the differences of the retrieved overlap functions are less sensitive to the guessed lidar ratio at the former wavelength, being in fact almost negligible. An overlap profile retrieved with the original noisy sequences (for LR = 50 sr) is plotted as well.

## 5. Conclusions

Based on same principle as in ref. (Wandinger and Ansmann, 2002). i.e. that the aerosol backscatter coefficient derived by the Raman method (Ansmann et al., 1992) is not affected by the lidar incomplete overlap (under the reasonable assumption of the same overlap function for the elastic and the Raman channels), a new formulation for deriving the overlap function of an aerosol lidar system equipped with Raman channels has been presented. As input data, the method uses the elastic and the Raman signals and a guess of the lidar ratio corresponding to the emitted wavelength of interest. The novelty of our approach consists in the derivation of an explicit formula in which no iterations have to be performed.

This formula allows one to assess the errors committed when an erroneous lidar ratio is used (section 3), showing, as already stated by (Wandinger and Ansmann, 2002), that the retrieval of the overlap function is less prone to errors when performed in clear atmospheres.

Results of the formula are illustrated with two examples, both with low aerosol load, but one of them with a much lower load than the other, showing the effect of the guessed lidar ratio on the overlap function retrievals.

## 6. Appendix: derivation of the explicit form of the overlap function

We outline here the mathematical details to obtain Eq. (15). Using the definitions of Eqs. (12), (13) and(14), Eq. (10) can be written as the Volterra integral equation

$$f(R) = g(R) + \phi(R)\int_R^{R_\infty} f(x)\psi(x)\,dx\,, \tag{A1}$$

which is amenable to a differential equation. In order to do that, we define the function

$$u(R) = \int_R^{R_\infty} f(x)\psi(x)\,dx\,, \tag{A2}$$

which, substituting into Eq. (A1), yields

$$f(R) = g(R) + u(R)\phi(R)\,. \tag{A3}$$

We next take the derivative Eq. (A2):

$$\frac{d}{dR}u(R) = -f(R)\psi(R) \tag{A4}$$

and substitute Eq. (A3) on it to obtain, after reordering terms

$$\frac{d}{dR}u(R) + \phi(R)\psi(R)u(R) = -g(R)\psi(R)\,. \tag{A5}$$

https://doi.org/10.5194/amt-2022-333
Preprint. Discussion started: 31 January 2023


Atmospheric Measurement Techniques Discussions

To integrate that equation, we define an integrating factor $\exp\left[\int_R^{R_m}\phi(x)\psi(x)\,dx\right]$ and multiply both members of Eq. (A5) by it, which allows us to recast the equation as

$$\frac{d}{dR}\left\{u(R)\exp\left[\int_R^{R_m}\phi(x)\psi(x)\,dx\right]\right\} = -g(R)\psi(R)\exp\left[\int_R^{R_m}\phi(x)\psi(x)\,dx\right]. \quad \text{(A6)}$$

Integrating both members of Eq. (A6) between $R$ and $R_m$, and noting that, by construction, $u(R_m)=0$, leads to

$$u(R) = \exp\left[\int_R^{R_m}\phi(x)\psi(x)\,dx\right]\int_R^{R_m} g(x)\psi(x)\exp\left[-\int_x^{R_m}\phi(x')\psi(x')\,dx'\right]dx. \quad \text{(A7)}$$

Finally, taking the derivatives of both members of Eq. (A7) and considering Eq. (A4) one obtains

$$f(R) = g(R) + \phi(R)\exp\left[\int_R^{R_m}\phi(x)\psi(x)\,dx\right]\int_R^{R_m} g(x)\psi(x)\exp\left[-\int_x^{R_m}\phi(x')\psi(x')\,dx'\right]dx \quad \text{(A8)}$$

## 7. Acknowledgements

The authors acknowledge the funding of this research by the Spanish State Agency for Research (AEI) for the project PID2019-103886RB-I00 and its support to ACTRIS ERIC. The authors also acknowledge the support of the European Commission through the Horizon 2020 Research and Innovation Framework Programme projects ACTRIS IMP (grant agreement No 871115), ATMO-ACCESS (grant agreement No 101008004) and GRASP-ACE (grant agreement No 778349).

## 8. References

Ansmann, A., Wandinger, U., Riebesell, M., Weitkamp, C. and Michaelis, W.: Independent measurement of extinction and backscatter profiles in cirrus clouds by using a combined Raman elastic-backscatter lidar., Appl. Opt., 31(33), 7113, doi:10.1364/AO.31.007113, 1992.

Comeron, A., Sicard, M., Kumar, D. and Rocadenbosch, F.: Use of a field lens for improving the overlap function of a lidar system employing an optical fiber in the receiver assembly, Appl. Opt., 50(28), 5538–5544, doi:10.1364/AO.50.005538, 2011.

Engelmann, R., Kanitz, T., Baars, H., Heese, B., Althausen, D., Skupin, A., Wandinger, U., Komppula, M., Stachlewska, I. S., Amiridis, V., Marinou, E., Mattis, I., Linné, H. and Ansmann, A.: The automated multiwavelength Raman polarization and water-vapor lidar PollyXT: The neXT generation, Atmos. Meas. Tech., 9(4), 1767–1784, doi:10.5194/amt-9-1767-2016, 2016.

Gimmestad, G. G. and Roberts, D. W.: Teaching lidar inversions, in Proceedings of the 25th International Laser Radar Conference, pp. 190–191., 2010.

Halldórsson, T. and Langerholc, J.: Geometrical form factors for the lidar function, Appl. Opt., 17(2), 240, doi:10.1364/AO.17.000240, 1978.

Klett, J. D.: Lidar inversion with variable backscatter/extinction ratios, Appl. Opt. Vol. 24, Issue 11, pp. 1638-1643, 24(11), 1638–1643, doi:10.1364/AO.24.001638, 1985.

Kokkalis, P.: Using paraxial approximation to describe the optical setup of a typical EARLINET lidar system, Atmos. Meas. Tech., 10(8), 3103–3115, doi:10.5194/amt-10-3103-2017, 2017.

Kumar, D. and Rocadenbosch, F.: Determination of the overlap factor and its enhancement for medium-size tropospheric lidar systems: a ray-tracing approach, J. Appl. Remote Sens., 7(1), 1–15, doi:10.1364/AO.50.005538, 2013.

https://doi.org/10.5194/amt-2022-333
Preprint. Discussion started: 31 January 2023




Kumar, D., Rocadenbosch, F., Sicard, M., Comeron, A., Muñoz, C., Lange, D., Tomás, S. and Gregorio, E.: Six-channel polychromator design and implementation for the UPC elastic/Raman lidar, edited by U. N. Singh and G. Pappalardo, p. 81820W, International Society for Optics and Photonics., 2011.

Lefrère, J.: Etude par sondage laser de la basse atmosphère, PhD Thesis, Universitè Paris 6, 1982.

Mathews, J. and Walker, R. L.: Mathematical Methods of Physics, 2nd ed., The Benjamin/Cummings Publishing Company., 1970.

Papoulis, A. and Pillai, S. U.: Probability, random variables, and stochastic processes, 4th ed., McGraw-Hill., 2002.

Sasano, Y., Shimizu, H., Takeuchi, N. and Okuda, M.: Geometrical form factor in the laser radar equation: an experimental determination, Appl. Opt., 18(23), 3908, doi:10.1364/ao.18.003908, 1979.

Sasano, Y., Browell, E. V. and Ismail, S.: Error caused by using a constant extinction/backscattering ratio in the lidar solution, Appl. Opt., 24(22), 3929, doi:10.1364/ao.24.003929, 1985.

Wandinger, U. and Ansmann, A.: Experimental determination of the lidar overlap profile with Raman lidar, Appl. Opt., 41(3), 511, doi:10.1364/ao.41.000511, 2002.

Zenteno-Hernández, J. A., Comerón, A., Rodríguez-Gómez, A., Muñoz-Porcar, C., D'amico, G. and Sicard, M.: A comparative analysis of aerosol optical coefficients and their associated errors retrieved from pure-rotational and vibro-rotational raman lidar signals, Sensors (Switzerland), 21(4), 1–21, doi:10.3390/S21041277, 2021.